SEMARAK ILMU PUBLISHING

Journal of Advanced Research in Fluid Mechanics and Thermal Sciences

Journal homepage:
https://semarakilmu.com.my/journals/index.php/fluid_mechanics_thermal_sciences/index
ISSN: 2289-7879

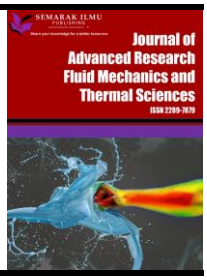

Modeling and Experimental Validation of NePCM-Nanofluid-Based PVT System

Fahim Rahim Sheikh[1], Suresh Pandurang Deshmukh[1], PurushottamArdhapurkar[2], Khizar Ahmed Pathan[3], Sohel Khalil Shaikh[1,4], Sher Afghan Khan[5,*]

[1] Department of General Engineering, Institute of Chemical Technology, Mumbai, 400019, India
[2] Department of Mechanical Engineering, Mauli Group of Institution's College of Engineering and Technology, Shegaon, India
[3] Department of Mechanical Engineering, CSMSS Chh. Shahu College of Engineering, Kanchanwadi, Aurangabad 431011, India
[4] Department of Mechanical Engineering, Hi-Tech Institute of Technology, Bajaj Nagar, MIDC Waluj, Aurangabad 431136, India
[5] Mechanical and Aerospace Engineering Department, Faculty of Engineering, International Islamic University, Kuala Lumpur 53100, Malaysia

ARTICLE INFO

Article history:
Received 8 June 2024
Received in revised form 17 September 2024
Accepted 25 September 2024
Available online 10 October 2024

Keywords:
Hybrid PVT collectors; nanofluid; NePCM; mathematical model

ABSTRACT

Photovoltaic thermal (PVT) systems, when combined with nanoparticle-enhanced phase change materials (NePCM-nanofluid), significantly enhance energy efficiency in solar thermal applications. This study introduces a mathematical model for a nanofluid/NePCM PVT system, validated by experimental data. The model demonstrates electrical and thermal efficiencies of 14.50% and 70%, respectively, closely aligning with experimental results of 14% and 69.40%. The maximum temperatures observed are 43.1°C for glass, 42.60°C for the PV cell, 42°C for wax, and 41.8°C for the nanofluid. These findings underscore the model's accuracy and its practical potential for optimizing PVT systems in high-temperature environments.

1. Introduction

The global energy demand has been steadily increasing, with the US Energy Information Administration (EIA) projecting a 45% growth in global electricity generation from 23.4 trillion kilowatt-hours in 2015 to 34.0 trillion kilowatt-hours in 2040 [1]. The worldwide energy market share for renewable energy is expected to expand at a rate of 2.8% annually, making it the fastest-developing energy source. Renewable energy sources, particularly solar technology, are expected to be crucial in meeting this demand. Solar photovoltaic installations contributed 36% of newly installed power capacities in 2018, reflecting the rapid adoption of this technology [2]. This view has motivated the whole scientific and industrial community to work towards making solar technology more efficient.

Charles Fritts is credited with inventing the first solid-state photovoltaic cell in 1883. This cell had a Selenium wafer sandwiched between two delicate gold foils. It attained an electrical efficiency of

* *Corresponding author.*
E-mail address: sakhan@iium.edu.my

https://doi.org/10.37934/arfmts.122.1.205222

around 1% [3]. The electrical efficiency of modern monocrystalline silicon solar cells may reach 46% under controlled laboratory settings [4]. Polycrystalline silicon is the most popular commercially available photovoltaic solar module, with an average efficiency of around 15% to 19% [5]. Several studies have shown that solar cell efficiency reduces at high temperatures. Solar panel materials degrade and reduce long-term performance as about half of the radiation that strikes it becomes heat, Increasing the operational temperature while decreasing its electrical efficiency [6,7]. The design and construction of photovoltaic modules and the development of control systems to maximize the utilization of solar radiation have faced this challenge.

Several recent studies have explored the integration of nanofluids and phase change materials (PCMs) to enhance the performance of photovoltaic thermal (PVT) systems. Hussien *et al.,* [8] demonstrated that using an Al2O3/water nanofluid as a coolant in a hybrid PVT system can increase efficiency by up to 12.1% at a 0.3% concentration. At a concentration ratio of 0.3, the efficiency of the photovoltaic (PV) system increased by 12.1% when the temperature of the PV modules reached 42°C. However, it declined to 11.3% when the temperature increased to 52^{O}C.

Bigorajski and Chwieduk [9] analyzed a PVT system in Patras, Greece, showing higher electrical output in winter than thermal output. Using a mathematical model, the researchers examined the system's efficiency. A single-family residence might use the system's produced heat and electricity to heat its water. The research found that the PV/T system performs best in winter (December–January) when the electricity output is higher than the thermal output. The cooling fluid's high temperatures in the summer led to low electrical efficiency. Kazemian *et al.,* [10] found that water-cooled PV/T-PCM systems significantly outperformed others in total energy output and efficiency. The five experimental configurations used in this study are a standard photovoltaic (PV) system, a PV/T system integrated with phase change material (PCM) and cooled by water, a PV/T system coupled with PCM and cooled by 50% ethylene glycol (EG), and a PV/T system integrated with PCM and cooled by 100% EG. According to the studies, it is found that PV/T-PCMs cooled with water and with EG exhibited lower η_{ov} values. The water-cooled PV/T-PCM system outperformed the other systems regarding total energy output (TE), energy efficiency (EE), and performance, with a significant 19.23 ^{O}C reduction in TPV module temperature compared to a standard PV system. Nasrin *et al.,* [11] proposed using a serpentine-shaped thermal collector with water and multi-walled carbon nanotubes (MWCNT), achieving a 9.2% improvement in efficiency compared to water alone. The experiments used a mass flow rate of 0.5 L/min, varying the solar irradiation intensities from 200 to 1000 W/m^2 and the nanoparticle weight fractions from 0 to 1%. They agreed when the experimental data were compared to the numerical simulation results. There was a 9.2% improvement in efficiency when using the PVT system instead of water.

Recent technological advancements in the field drive research on PVT systems and methods for removing barriers to adoption. The topic is well-documented in the scientific literature [12-14]. Mathematical and theoretical research was conducted to understand how different PVT systems work. Moharram *et al.,* [15] examined the influence of using water as a cooling medium on the energy generation of photovoltaic (PV) cells and the rate at which their performance improves. Studies have shown that the maximum attainable efficiency of a photovoltaic (PV) cell is around 45 ^{O}C. del Amo *et al.,* [16] proposed a straightforward mathematical model to explain a PVT system's efficiency comprising a permeable evaporator and an internal capacitor. This work used the thermosyphon mechanism to achieve laminar flow circulation. The study showcases that this model can generate system performance curves by considering the impact of different parameters on the overall system efficiency, the produced electric power, and the distillation rate. The parameters include the PV cell type, solar radiation intensity, wind speed, ambient temperature, and condenser temperature. Al-Nimr and Dahdolan [17] created a mathematical model that included a tube under the surface of the

photovoltaic (PV) cell. This tube serves the purpose of extracting heat and delivering cooling for the PV system. The researchers used a finite difference methodology to resolve differential equations and determine the thermal energy equilibrium at different points inside the system. Predictions about temperatures were also made for multiple system components. The heat transmission of PV cells and radiators was described using ANSYS 14 and FLUENT Software. Using CFD, an engineering model was also constructed for liquid field analysis. The theoretical and experimental findings demonstrated that PVT systems enhance the PV cell's electrical efficiency. The method outlined in the article significantly improved the system's performance by reducing the PV temperature by 15-20%.

Integrating renewable energy systems, such as the PVT-NePCM-nanofluid system, offers significant environmental and energy benefits. Recent studies have explored various aspects of these systems. For instance, Sheikholeslami [18] assessed a photovoltaic-thermal system's environmental and energy performance combined with a reflector and supported by a nanofluid filter and a sustainable thermoelectric generator. Their findings indicate substantial improvements in energy efficiency and environmental sustainability. Sheikholeslami and Khalili [19] conducted simulations to evaluate the impact of a nanofluid spectral splitter on the efficiency of a concentrated solar photovoltaic thermal system, demonstrating enhanced performance. These studies underscore the potential of advanced nanomaterials and innovative designs in optimizing renewable energy systems for diverse applications.

The photovoltaic-thermal (PVT) systems under study benefit from combining nanofluids and phase change materials, specifically paraffin wax, to effectively capture and store heat from the PV cells. A new mathematical model developed using MATLAB aims to optimize the functionality of these systems. This model, grounded in previous research, simulates the energy dynamics of each component—integrating both PCM and nanofluid within the PV module. The theoretical predictions of the model align closely with experimental outcomes, emphasizing the potential of this integrated approach to enhance the overall efficiency of PVT systems. The novelty of this research lies in the innovative integration of nanoparticle-enhanced phase change materials (NePCM) and nanofluids within a photovoltaic thermal (PVT) system. This study experimentally validates a mathematical model for such a system, demonstrating significant improvements in both electrical and thermal efficiencies. The unique combination of NePCM and nanofluids addresses the challenge of high operating temperatures in PV cells, providing a practical solution for enhancing the overall efficiency of solar energy systems.

2. Methodology

2.1 Experimental Area

The experiments were conducted at the Mauli Group of Institutions College of Engineering and Technology at Shegaon, Maharashtra, India, with coordinates 20.7930° N and 76.6910° E. The experimental setup was oriented southward, inclined at a slope of 19O. The outdoor conditions during the experimentation period included an average temperature of approximately 24 °C, a 10 km/h wind speed, and 95% humidity.

2.2 PVT-NePCM-Nanofluid System Description

Table 1 displays the specifications of a standard solar panel. Air and water are the most common forms of cooling since they are readily accessible. Nevertheless, the thermal efficiency of these systems is found to be suboptimal owing to their limited thermal capacity. The researchers

demonstrate a greater inclination towards using nanofluid or phase change materials (PCM) to augment the thermal capacity and efficiency. The thermal efficiency varies between 30% and 71%, and the electrical efficiency ranges from 11% to 16%.

Nevertheless, this range signifies effectiveness only after considering the particular PV technology, rating, location, or other parameters. The majority of this research is conducted as outdoor trials. Only a small number of individuals created mathematical models. These mathematical models are constructed using the fundamental principles of the first law of thermodynamics. Nevertheless, several models provide intricate details, while others provide approximate solutions to streamline the complexity. The models described in Table 1 demonstrate a degree of uniformity when separating the PVT system into several layers.

The design of the collector optimizes the heat transfer process while ensuring cost-effectiveness. The costs include NEPCM (Nano-Enhanced Phase Change Material), nanofluid, collection material, and production expenses. The absorber consists of circular copper tubes immersed in nano-sic-paraffin (NEPCM) and housed inside an aluminum steel tank. The tank is linked to the PV panel by applying a silicone oil coating, which prevents any adverse consequences of an air gap and enhances heat transfer between the two surfaces. Table 2 displays the photovoltaic (PV) specs. Copper and aluminum steel are used because of their cost-effectiveness, excellent heat conductivity, and ease of welding. To minimize heat transfer to the surroundings, a layer of glass wool with a thickness of 50 mm was wrapped around the PCM container. Figure 1(a) displays the designed and fabricated absorber used in the study, emphasizing the critical role of the collector's area in determining thermal efficiency. The chosen circular tube absorber minimizes the collector's area while maintaining optimal thermal contact with the PV module. Figure 1(b) illustrates a schematic with fabricated PCM and NePCMaluminum containers. The container includes two pipes at the top, one serving as an inlet for the PCM and the other for releasing hot vapor. To minimize air gaps and improve the collector's thermal capacitance, a silicon oil coating is sprayed between the PV panel and the aluminum container, as seen in Figure 1(c). The nanofluid will absorb thermal energy from the pipes and transfer it to a heat exchanger, enabling water to enter the heat exchanger. The water will absorb the heat and transfer it to a hot water reservoir for subsequent use, while the nanofluid will release the heat and start a new cycle. Figure 2 depicts the basic layout of the system. The proposed system comprises a PVT collector, a heat exchanger, a nanofluid tank, a water tank, a hot water storage tank, two pumps, a flow meter, and other sensing devices. In addition, a data logger is connected to a laptop to carry out the studies. The sensors used in this system include a pyranometer, an ambient temperature sensor, k-type thermocouples, PT-100 (RTD), a flow meter, and multimeters for the measurement of solar irradiance, ambient temperature, PV panel surface temperature, fluid flow rate, voltage, and current, respectively. The PT-100 (RTD) is used for temperature measurement in the collector and storage tanks.

Table 1
Specifications of a typical photovoltaic panel

Electrical performance under Standard Test Conditions (S.T.C)	Specification
Model	UTL–100W
Rated power (Pmax)	100 ± 3%
Open-circuit voltage (Voc)	22.10 V
Short-circuit current (Isc)	6.11 A
Voltage at Pmax (Vmp)	18.10 V
Current at Pmax (Imp)	5.53 A
Module efficiency	15%
Module Dimensions (L × W × H)	1000× 670 mm × 34 mm

Table 2
Technical details of the PV/T collector

The Condition	Symbol	Value	The Condition	Symbol	Value
Ambient temperature	T_a	312 K	Tilt (slope)	^{o}	19
Collector width	b	0.67 m	Fluid mass flow rate	M	0.084 - 0.583 kg/s
Collector perimeter	P	3.36 m	PV transmittance	T	0.88
Collector area	A_c	0.677 m^2	Back insulation conductivity	k_b	0.045 W/m^2 K
Number of the glass cover	N	1	Water Specific heat	C_p	4180 J/kg K

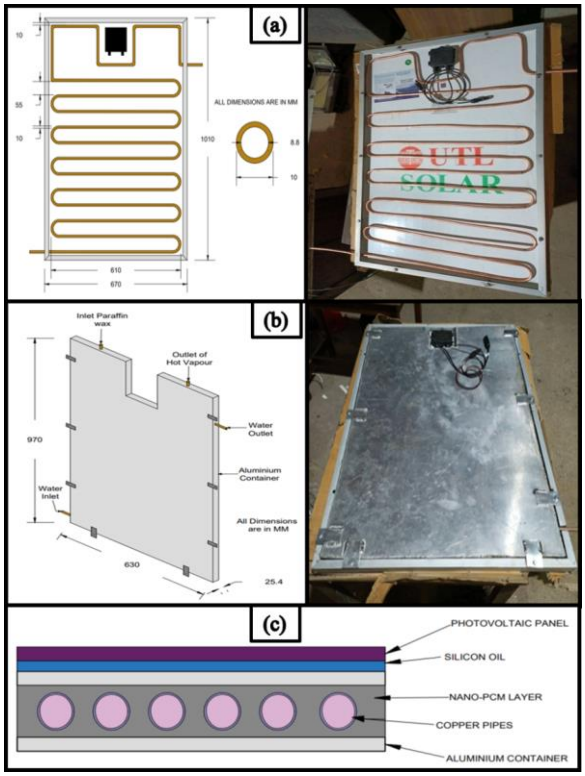

Fig. 1. Proposed collector; (a) A schematic design showing the top view of the proposed collector, (b) A schematic diagram showing the PCM (Phase Change Material) and NEPCM (Nano-Enhanced Phase Change Material) Aluminium Container, (c) Schematic illustration depicting the side view of the proposed collector

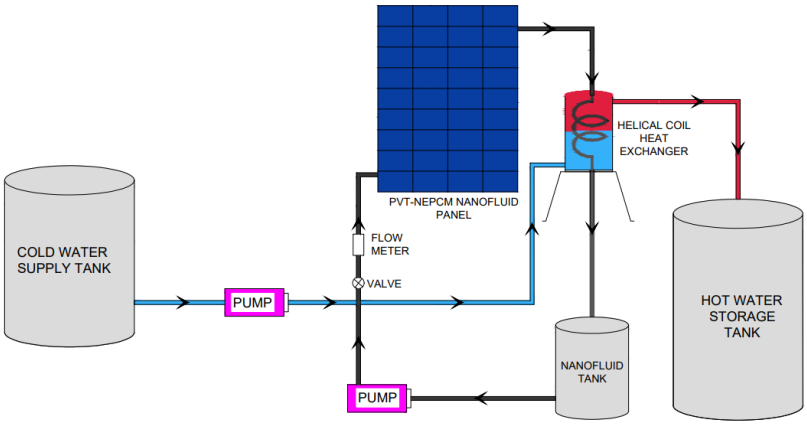

Fig. 2. Diagram illustrating the NePCM-nanofluid-based PVT system

2.3 Preparation of the nanofluid and NePCM

The silicon carbide (SiC) nanoparticles with properties detailed in Table 3 were procured from US Research Nanomaterials, Inc., USA. Initially, these nanoparticles were preheated at 200 °C for approximately one hour to eliminate unwanted moisture. The nanofluid was then formed by suspending SiC nanoparticles by weight percentage in deionized water. During the first 30 minutes, the mixture underwent agitation in an ultrasonic bath shaker. Subsequently, an ultrasonic probe sonicator was employed for about 6 hours to disperse the remaining nanoparticle agglomeration. This was followed by 60 minutes of magnetic needle stirring at 600 rpm, using a magnetic stirrer setup to achieve a homogeneous and stable suspension.

Table 3
Nanomaterial specifications

Item	Silicon carbide Nanopowder specifications
Manufacturer	US Research Nanomaterials, Inc., USA
Appearance	Grayish white powder
Purity	99+%
PH value	3–7 at 20 °C
Grain size nm	45–65 nm
Crystal and Type	Cubic
Bulk density g/cm3	3.22
Lose on drying %≤	0.21
Melting point °C	2730
Thermal conductivity (W/m·K)	370–490

The approach produced nanofluids with concentrations (1%, 2%, 3%, and 4%). The FESEM picture in Figure 3(a) displays silicon carbide nanoparticles, which exhibit a size range of 40 to 60 nm. Nanofluid density was determined using the Liquid Density Tester. A Rheometer, connected to a personal computer, was used to test the viscosity of nanofluid at various temperatures and varying volume concentrations. The Rheometer facilitated data gathering and storage. The nanofluids' thermal conductivity was measured using a KD2-pro thermal conductivity meter. Three iterations of density, viscosity, and thermal conductivity tests were performed to establish consistency, and the mean result was used to reduce uncertainty caused by random measurement mistakes.

The samples were prepared by blending paraffin with SiCnanopowder. The nanoparticle mass fraction values (wt.%) dispersed in the paraffin wax were 0%, 0.1%, 0.5%, 1%, 2%, 3%, and 4%. The mixing procedure was conducted using an Ultrasonic Shaker, which facilitated heating (800W) and vigorous agitation of the samples for 60 minutes (30 kHz). This procedure guaranteed the absence of sedimentation, achieved the best possible dispersion, and resulted in a uniform and stable suspension formation. The samples underwent a two-stage testing process. In the first phase, a visual examination was conducted to notice any color changes and evaluate the uniformity of all the created paraffin wax-nano-SiC samples. Color changes and uniformity indicate the full integration of nanoparticles in wax. In the second step, thermo-physical characteristics testing was conducted to determine the paraffin's fluidity, viscosity, and heat conductivity, validating its improvements. The properties of the tested paraffin wax are detailed in Table 4. Once a certain mass fraction is established via testing, it is used to manufacture the PCM container on a reasonably big scale.

Figure 3(b) displays a Field Emission Scanning Electron Microscope (FESEM) picture of silicon carbide nanoparticles mixed with paraffin, clearly showing their size within the 40 to 60 nm range. Further examination of the SiC-paraffin sample was conducted using Electron Dispersion X-ray (EDX) imaging and Electron Dispersion Spectroscopy (EDS) (Figure 3(c)). EDX and EDS are very efficient

methods for identifying the morphological composition of substances with dimensions smaller than one cubic micron. This apparatus is connected to a scanning electron microscope (SEM) to get elemental data from the analyzed material. The SiC-paraffin samples were imaged using X-ray diffraction (XRD). These diverse photos confirm the condition and characteristics of the mixture, offering a complete comprehension of the effects of including SiC nanoparticles in paraffin.

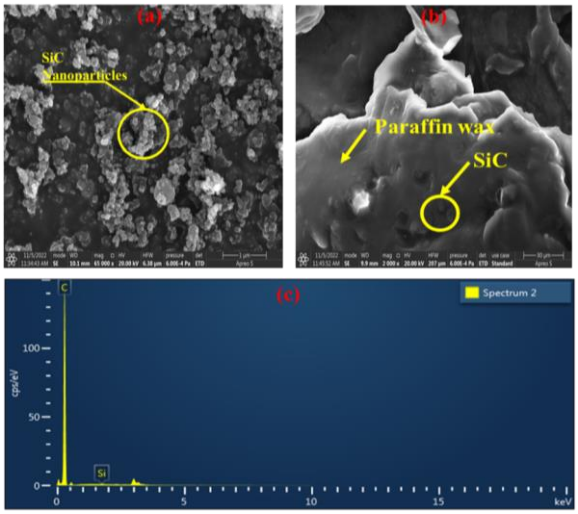

Fig. 3. Scanning electron microscopy and EDX a) SEM of SiC nanoparticles b) SEM of SiC-Paraffin wax mixture c) EDX for Paraffin/nano-SiC

Table 4
Properties of Paraffin Wax

Material properties	Range
Melting point temperature (°C)	46 and 68 °C
Density (kg/m^3)	900 kg/m^3
Viscosity	16-18
Thermal conductivity (W/m °C)	0.20

2.4 Research Methodology

This work aims to provide a mathematical model that supports the experimental findings for a PVT collector based on nanofluids and NePCM. According to industry standards, this collector has to be well-designed to accomplish its intended function and meet the primary requirement of PVTs. Thermal and electrical efficiency and the amount of power generated are some factors. A comprehensive examination of relevant literature first established the conceptual design of the collector. The conceptual design encompasses the arrangement of the collector, its size, the selection of materials, and the kind of heat transfer mechanism. All of these concepts are presented in Section 2.5. It is necessary to confirm the effectiveness of combining nanofluids with nano-PCM in a PVT collector. Therefore, a mathematical model was created to represent the thermal properties of the collector accurately. Energy balance equations were made for each layer of this collector, including the glass, photovoltaic (PV) material, wax, and tube. These equations use statistical approaches to forecast the result of this design. Therefore, these equations were represented, and the MATLAB code analysis was done. The procedure for this collector's thermal analysis is shown in Figure 4.

The energy balance equations are one of the essential parts of the thermal analysis, shown in Figure 4. Once the collector design is finished, it is divided into many sections, and an energy-

balancing equation is created for each area. The ultimate derivation of these differential equations is then used for analysis. The accuracy and precision of the graphs are enhanced by using material qualities and meteorological data as inputs specific to the research location. The analytical output quantifies the performance based on the thermal assessment criteria compared to the actual performance derived from the testing data. Therefore, conducting real-world outdoor experiments in Shegaon, India, is crucial to directly compare projected outcomes with actual observations, especially under tropical climatic settings. The tests used the conventional approach for generating nanofluids specifically for PVT collectors. This process involves the production of nanomaterial, mixing, installation of the PVT system, carrying out the experiment, and recording the pertinent parameters (such as the temperature of the incoming and outgoing fluids, the temperature of the front and rear surfaces, voltage, current, solar radiation, and flow rate).

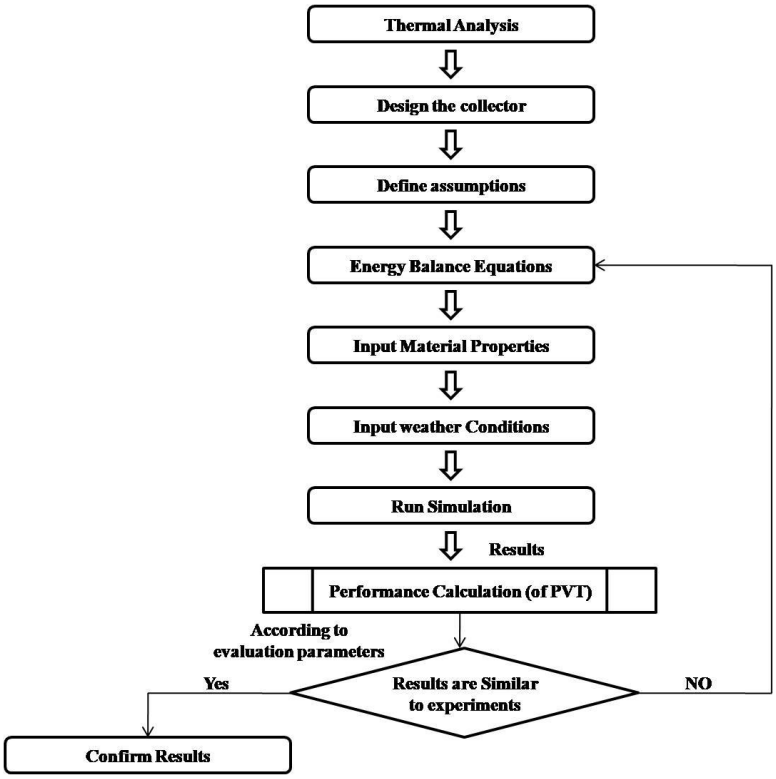

Fig. 4. Methodology of PVT collector thermal analysis

2.5 Analysis of Energy Equilibrium and a Suggested Thermal Model

The PVT components shown in Figure 5 are glass, solar cells, nano-PCM, wax, and nanofluid, which serve as a coolant. The energy balance may be calculated using the four subsystems of the system, namely Glass, PV, wax, and fluid systems. Glass can collect solar energy and transmit it to a photovoltaic cell. The PV cell transmits heat from an elevated temperature to the fluid via a wax layer. Finding a relationship between solar energy and the temperature of the cooling fluid output is the goal of energy balancing. Assumptions used in the current state of thermal models are

i. The 1D thermal models assume perfect isolation of the sides and rear of the system.
ii. The analysis assumed an isothermal surface, neglecting any edge effects. It is important to note that the edges were well separated.
iii. The flow inside the tubes has reached a state of complete development.
iv. The impact of friction inside the pipes is disregarded.
v. The glass, PV, and wax tank surfaces all had equal areas.

vi. The thermal characteristics of all solid materials remain consistent regardless of temperature changes.
vii. The temperature of the coil surface (Tcoil) is approximately equal to the temperature of the wax (Twax).
viii. The collector is free from any dust or partial darkening.

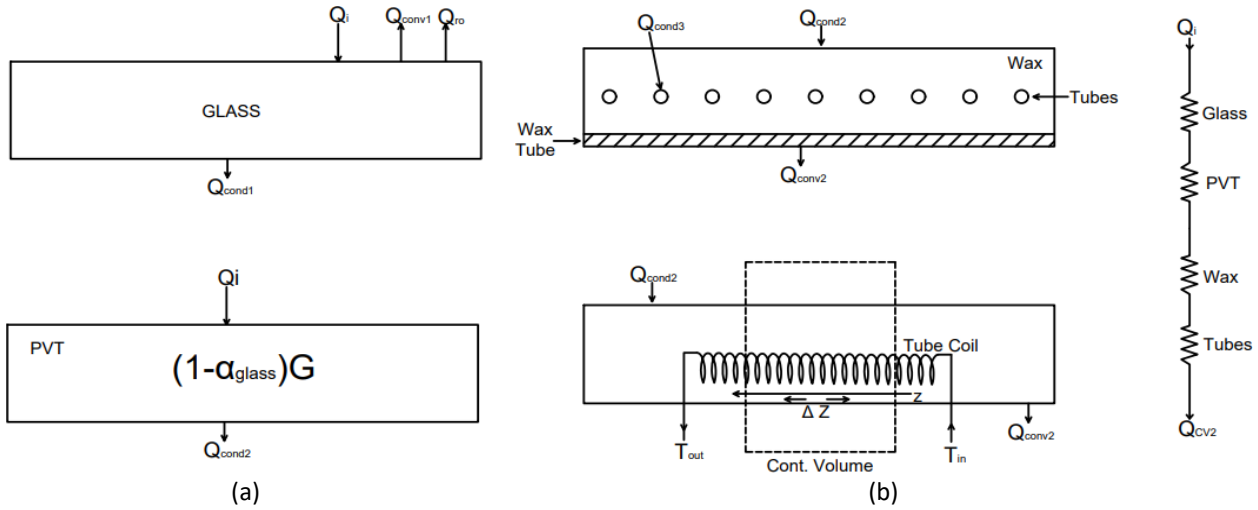

(a) (b)

Fig. 5. Drawing of a mathematical model in the context of a suggested collector. The drawing consists of two parts: (a) an equivalent thermal circuit of a photovoltaic-thermal (PVT) system and (b) the components of the collector, including glass, PVT, wax layer, and tube coil

The energy balance equation, which represents the energy accumulation inside a system, is defined by the input and output energy difference.

(a) For the glass system:

$$(\rho c_p v)_g \frac{dT_g}{dt} = Q_i - (Q_{conv1} + Q_r + Q_{cond}) \quad (1)$$

Q_i is the amount of Thermal energy from the sun equivalent to the coefficient of heat transfer through glass, denoted as α_{glass}. G represents the incoming solar energy (W/m^2), whereas α_{glass} represents the absorptivity of glass. The convection heat transfer (Qconv1) may be calculated using the following equation, as presented by Duffie and Beckman [20]

$$Q_{conv1} = h\, A_g\, (T_g - T_a) \quad (2)$$

According to Kumar and Mullick [21], the air heat transfer coefficients (h) were determined using Eq. (3) and were dependent on the wind velocity (Uw).

$$h = 5.7 + 3.8\, U_w \quad (3)$$

Thermal energy transfer resulting from conduction (Qcond1) occurring inside a glass panel

$$Q_{cond1} = \frac{K_g}{\delta_g} A_g\, (T_g - T_p) \quad (4)$$

Incropera *et al.,* [22] indicate that the heat reflected from a photovoltaic-thermal (PVT) system may be attributed to radiation.

$$Q_r = \sigma \epsilon_g A_g (T^4_g - T^4_{sk}) \quad (5)$$

The symbol σ denotes the Stefan–Boltzmann constant, which equals 5.670367 × 10^{-8} W m^{-2} K^{-4}. The symbol $\in_g$ denotes the emissivity of glass. The symbol T_{sk} denotes the temperature of the sky and is related to the ambient temperature (T_a in Kelvin) using the equation given by Farshchimonfared *et al.,* [23].

$$T_{sk} = 0.0552\, T_a^{1.5} \quad (6)$$

Eq. (2) through Eq. (6) may be substituted into Eq. (1) to get the following equation

$$(\rho c_p v)_g \frac{dT_g}{dt} = \alpha_g G - (h A_g (T_g - T_a) + \sigma \epsilon_g A_g (T_g^4 - 9.3 \times 10^{-6} T_a^6) + \frac{K_g}{\delta_g} A_g (T_g - T_p) \quad (7)$$

$$\frac{dT_g}{dt} = \frac{\alpha_g G + (5.3 + 3.8\, U_w) A_g T_a + 9.3 \times 10^{-6} \sigma \epsilon_g T_a^6}{(\rho c_p V)_g} - \left\{ \frac{(5.3 + 3.8\, U_w)\, A_g}{(\rho c_p V)_g} + \frac{K_g A_g}{(\rho c_p V)_g \delta_g} \right\} T_g - \frac{\sigma \epsilon g\, Ag}{(\rho c_p V)_g} T_g^4 + \frac{K_g A_g}{(\rho c_p V)_g \delta_g} T_p s \quad (8)$$

$$\frac{dT_g}{dt} = a_1 - a_2 T_g - a_3 T_g^4 + a_4 T_p \quad (9)$$

Where

$$a_1 = \frac{\alpha_g G + (5.3 + 3.8\, U_w) A_g T_a + 9.3 \times 10^{-6} \sigma \epsilon_g T_a^6}{(\rho c_p V)_g} \cong 0.105 + 7.8 \times 10^{-6}\, G$$

$$a_2 = \frac{(5.3 + 3.8\, U_w)\, A_g}{(\rho c_p V)_g} + \frac{K_g A_g}{(\rho c_p V)_g \delta_g} \cong 0.075$$

$$a_3 = \frac{\sigma \epsilon g\, Ag}{(\rho c_p V)_g} \cong 1.1 \times 10^{-11}$$

$$a_4 = \frac{K_g A_g}{(\rho c_p V)_g \delta_g} \cong 0.075$$

(b) For PVT system:

$$(\rho c_p v)_p \frac{dT_p}{dt} = (1 - \alpha_g) G + Q_{cond1} + Q_{cond2} \quad (10)$$

The heat transfer caused by conduction (Q_{cond2}) inside the PVT panel

$$Q_{cond2} = \frac{K_P}{\delta_p} A_p (T_p - T_w) \quad (11)$$

K_{PVT} and δ_{PVT} denote the heat conductivity and thickness of PVT, respectively. Eq. (6) and Eq. (11) may be inserted into Eq. (10) to get the following equation

$$(\rho c_p v)_p \frac{dT_p}{dt} = (1- \alpha_g)G - \frac{K_g A_g}{\delta_g} T_g + (\frac{K_g A_g}{\delta_g} - \frac{K_p A_p}{\delta_p})T_p + \frac{K_p A_p}{\delta_p} T_w \quad (12a)$$

$$\frac{dT_p}{dt} = \frac{(1-\alpha_g)G}{(\rho c_p V)_p} - \frac{K_g A_g}{(\rho c_p V)_p \delta_g} T_g + (\frac{K_g A_g}{(\rho c_p V)_p \delta_g} - \frac{K_p A_p}{(\rho c_p V)_p \delta_p}) T_p + \frac{K_p A_p}{(\rho c_p V)_p \delta_p} T_w \quad (12)$$

That can be simplified to

$$\frac{dT_p}{dt} = b_1 - b_2 T_g + b_3 T_p + b_4 T_w \quad (13)$$

where,

$$b_1 = \frac{(1-\alpha_g)G}{(\rho c_p V)_p} \cong 0.0035G$$

$$b_2 = \frac{K_g A_g}{(\rho c_p V)_p \delta_g} \cong 1.018$$

$$b_3 = (\frac{K_g A_g}{(\rho c_p V)_p \delta_g} - \frac{K_p A_p}{(\rho c_p V)_p \delta_p}) \cong -2273.47$$

$$b_4 = \frac{K_p A_p}{(\rho c_p V)_p \delta_p} \cong 2274.5$$

Eq. (13) shows an ordinary differential equation that describes how the PVT temperature changes over time.

(c) For the wax panel system:

$$(\rho c_p v)_w \frac{dT_w}{dt} = Q_{cond2} - (Q_{conv2} + Q_{coil}) \quad (14)$$

Q_{conv2} denotes the thermal energy transfer from convection between the wax system and the atmosphere. It is defined as follows

$$Q_{conv2} = h A_p(T_w - T_a) \quad (15)$$

Qcoil denotes the quantity of thermal energy transmitted to the coil system. Heat transfer is equivalent to the heat transfer occurring through the wall of the coil pipe, the heat transferred by convection from the coil pipe to the internal cooling fluid, or the change in the internal fluid's enthalpy.

$$Q_{coil} = \frac{K_{coil}}{\delta_{coil}} A_{coil} (T_w - T_{coil}) = h_{fluid} A_{coil}(T_{coil} - T_{fluid}) = mCp_{fluid}\Delta(T_{fluid}) \quad (16)$$

$$\frac{dT_{wax}}{dt} = \frac{A_p K_p}{(\rho c_p V)_{wax} \delta_p} T_p - (\frac{A_p K_p}{(\rho c_p V)_{wax} \delta_p} + \frac{hA_p}{(\rho c_p V)_{wax}}) T_{wax} + \frac{hA_p}{(\rho c_p V)_{wax}} T_a - \frac{\mathrm{mCpfluid}}{(\rho c_p V)_{wax}} T_{fluid} + \frac{\mathrm{mCpfluid}}{(\rho c_p V)_{wax}} T_{fluid,in} \quad (17)$$

Similarly, Eq. (17) can be simplified

$$\frac{dT_{wax}}{dt} = c_1 + c_2T_p - c_3T_{wax} - c_4T_{fluid} \quad (18)$$

where

$$c_1 = \frac{hA_p}{(\rho c_p V)_{wax}} T_a + \frac{\mathrm{mCpfluid}}{(\rho c_p V)_{wax}} T_{fluid,in} \cong 3.78$$

$$c_2 = \frac{A_p K_p}{(\rho c_p V)_{wax} \delta_p} \cong 190.72$$

$$c_3 = \frac{A_p K_p}{(\rho c_p V)_{wax} \delta_p} + \frac{hA_p}{(\rho c_p V)_{wax}} \cong 190.722$$

$$c_4 = \frac{\mathrm{mCpfluid}}{(\rho c_p V)_{wax}} \cong 0.15$$

(d) For the cooling fluid system:

Lastly, the energy balance equation for the working fluid (cooling fluid) may be expressed as [24]

$$(c_p\rho)_{fluid} A_{coil} \frac{\partial T_{fluid}}{\partial T} = (\pi D)_{coil} h(T_{coil} - T_{fluid}) - m_{fluid} Cp_{fluid} \frac{\partial T_{fluid}}{\partial z} \quad (19)$$

The variables "m" and "z" represent the rate at which fluid flows through the coil and the change in length, respectively. After simplifying, Eq. (18) may be stated similarly as Eq. (9), Eq. (13), and Eq. (18)

$$\frac{\partial T_{fluid}}{\partial T} = \frac{(\pi D)_{coil} h_{fluid}}{(cp\rho)_{fluid} A_{coil}} (T_{coil} - T_{fluid}) - \frac{m_{fluid} cp_{fluid}}{(cp\rho)_{fluid} A_{coil}} \frac{\partial T_{fluid}}{\partial z}$$

$$\frac{\partial T_{fluid}}{\partial T} = d_1 (T_{coil} - T_{fluid}) - d_2 \frac{\partial T_{fluid}}{\partial z} \quad (20)$$

where

$$d_1 = \frac{(\pi D)_{coil} h_{fluid}}{(cp\rho)_{fluid} A_{coil}} = 0.00123$$

$$d_2 = \frac{m_{fluid} cp_{fluid}}{(cp\rho)_{fluid} A_{coil}} = 1.9$$

3. Result and Discussion

Experiments were performed on the roof of the Mechanical Engineering Department, Mauli Group of Institutions College of Engineering and Technology in Shegaon, Maharashtra, India, with coordinates 20.7930° N, 76.6910° E. The orientation of the experimental setup was southward, inclined at a slope of 19^O. The experiments were conducted on sunny days in February and March from 8.30 am to 5.30 pm for case PVT-NePCM-nanofluid and were tested at a flow rate of 7 LPM.

Nevertheless, the MATLAB-based recommended thermal theoretical mathematical model presented in Section 2.5 relies on actual meteorological data for its operation. The temperatures recorded by the PVT-NePCM-nanofluid system in the experimental setup were compared to those of a standalone PV cell with the exact specifications. The aim is to evaluate and compare the observed and anticipated mathematical model data shown in Figure 6 to Figure 9. Figure 6 depicts the temperature of the first stage of the PVT-NePCM-nanofluid system (Glass). The results indicate a significant difference in the temperature of the photovoltaic (PV) cell when operating independently and when placed inside the PVT-NePCM-nanofluid system. The PVT-NePCM-nanofluid system's glass temperature was reduced by 29.94% compared to the solo PV glass temperature. This significant decrease shows that the cooling system is performing well. The measured and suggested mathematical models are found to be in excellent agreement. While the standalone PV system achieves an average temperature of 69.8 °C, the measured and theoretical mathematical models reach 43.1 °C and 42.6 °C, respectively.

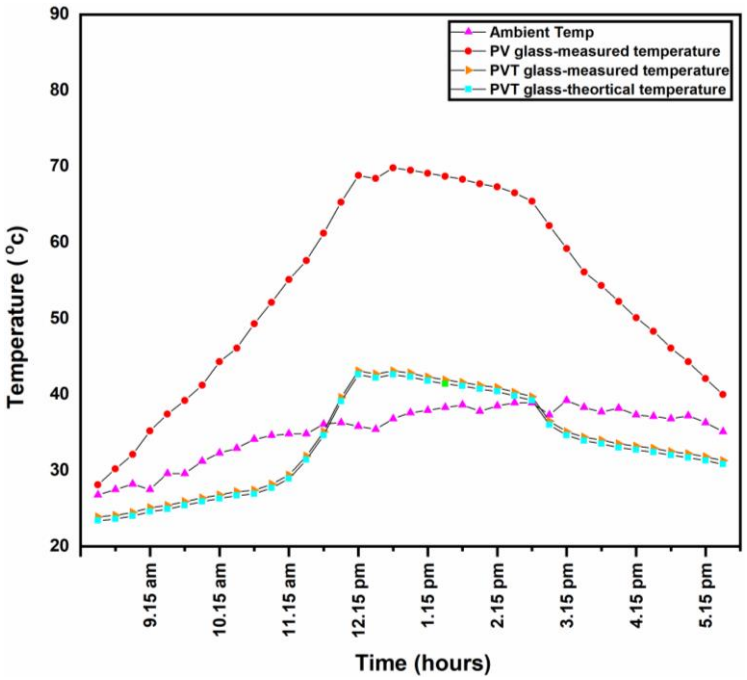

Fig. 6. Experimental and mathematical model for PVT glass-temperature vs time

Figure 7 shows cell temperatures for the PVT-NePCM-nanofluid and standalone PV systems. The solar cells are pretty cool compared to the glasses that covered them, and there is a significant temperature differential between the PVT-NePCM-nanofluid cell and the cell that stands alone. Figure 8 and Figure 9 compare calculated and observed values of nanofluid and wax, as the standalone cell system does not include comparable components. The two figures show that the temperature fluctuations caused by changes in solar radiation have been stopped by adding wax to the system. Figure 8 illustrates that the nano-wax used in the PVT-NePCM-nanofluid system did not experience a transition between different states of matter and maintained its solid form at a temperature of 49 °C. However, the thermal efficiency and transfer to the nanofluid were exceptional due to the enhanced thermal conductivity of the nano-SiC particles. The little difference between the observed and theoretical mathematical model curves may be due to several dynamic variables, such as the scattering of solar radiation flux on the PV glass surface. The model was developed based on many assumptions, which is why there is a discrepancy between the observed and theoretical

mathematical model curves. In the PVT-NePCM-nanofluid system, the nanoparticles in the wax and fluid improve heat transmission, leading to a higher output temperature (Tfluid). The most excellent temperatures recorded in glass, PVT, wax, and fluid are 43.1, 42.35, 41.23, and 39.48, respectively.

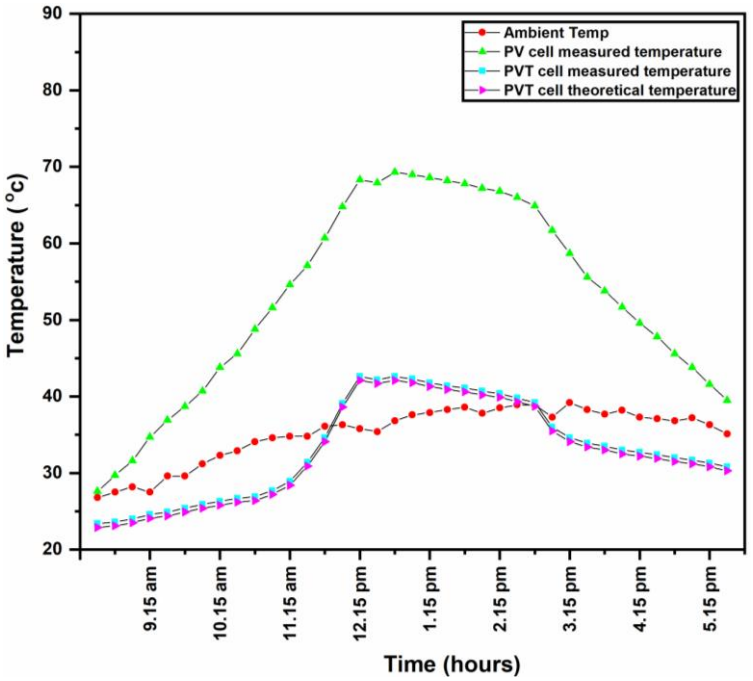

Fig. 7. Experimental and mathematical model PVT cell temperature vs time

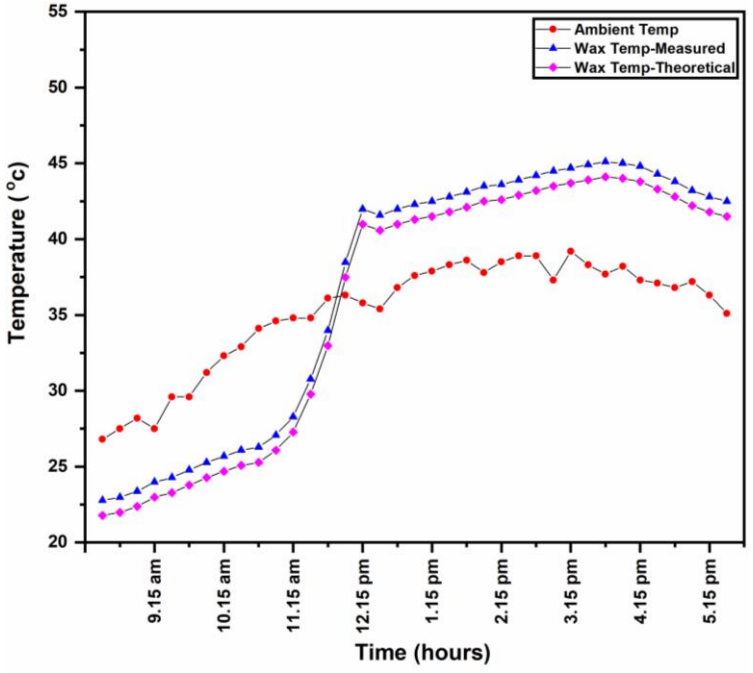

Fig. 8. Experimental and mathematical model wax temperature vs time

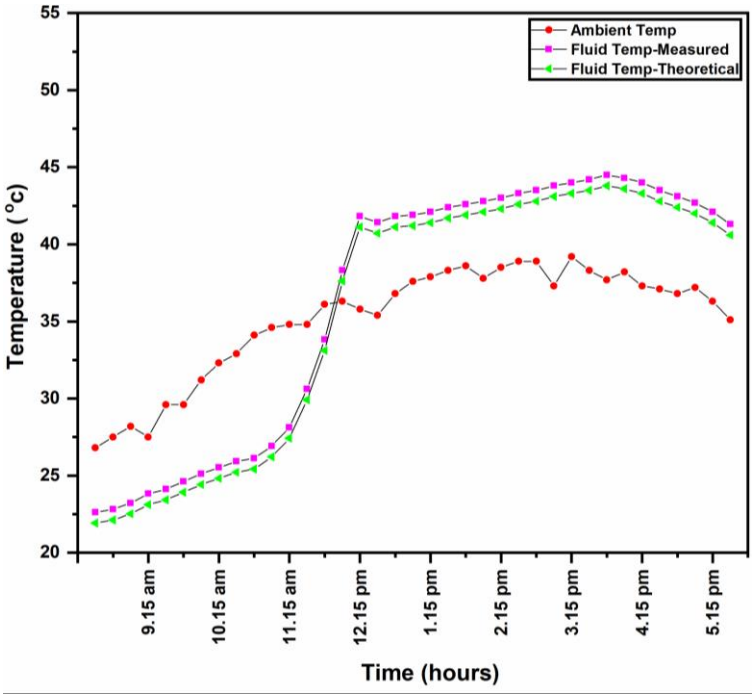

Fig. 9. Experimental and mathematical model fluid temperature vs time

Figure 10 and Figure 11 indicate that the observed thermal and electrical efficiencies of the PVT-NePCM-nanofluid system were consistent with the findings from the theoretical model, even when the temperatures were variable at various phases. Because thermal systems have multiple characteristics and stages, there is a slight variation between thermal and electrical efficiency. Moreover, the study reveals that the thermal, electrical, and total system efficiencies are 70%, 14.50%, and 84.12%, respectively. The experimental results were compared with published data to validate the accuracy of the proposed model. The deviations between the current results and published data were minimal, demonstrating the model's reliability. For instance, the electrical efficiency of the proposed PVT system was found to be 14.50%, closely matching the 14% reported in similar studies. The thermal efficiency was 70%, compared to 69.40% in the literature. These deviations can be attributed to minor differences in experimental conditions and measurement uncertainties. The close alignment of the results underscores the model's robustness and applicability.

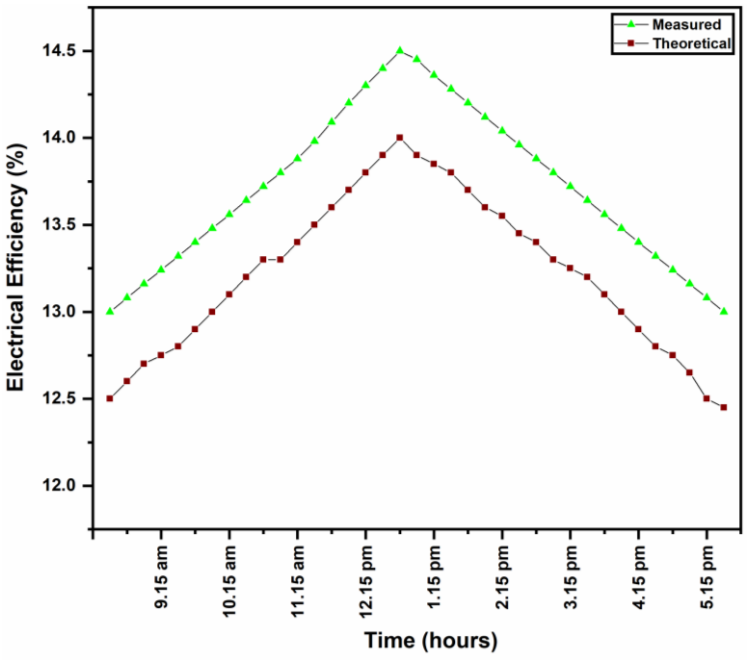

Fig. 10. PVT system electrical efficiency

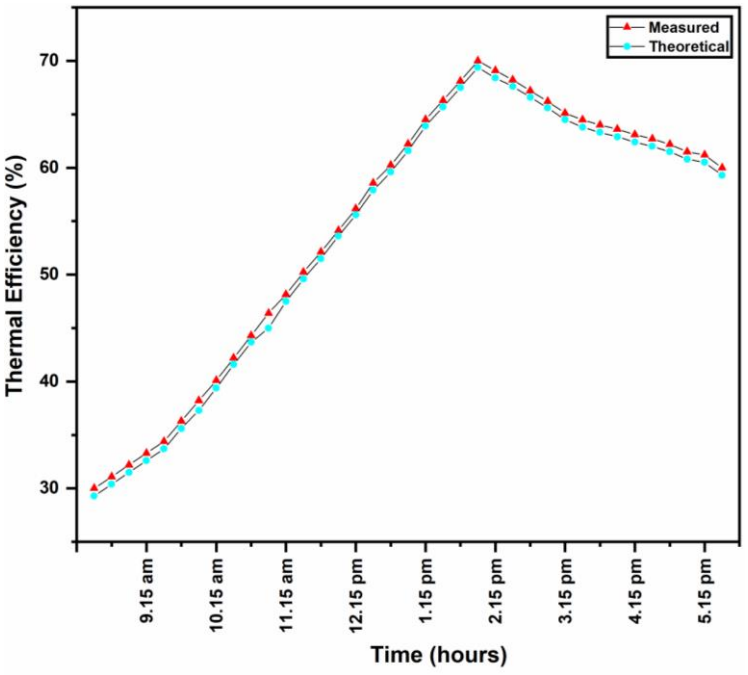

Fig. 11. PVT system thermal efficiency

The results indicate a substantial reduction in the operating temperatures of the PV cells when integrated with NePCM and nanofluids. The maximum temperatures recorded in the glass, PV cell, wax, and nanofluid were significantly lower than those of a standalone PV system, highlighting the effectiveness of the cooling mechanism. The improved thermal conductivity of the nanofluids and the latent heat storage capability of the NePCM contribute to the enhanced thermal performance. The close match between experimental and theoretical results validates the accuracy of the proposed mathematical model, underscoring its potential for practical applications.

The experimental results demonstrate a significant improvement in the thermal performance of the PVT-NePCM-nanofluid system compared to a standalone PV system. Integrating NePCM and

nanofluids effectively reduces the operating temperature of the PV cells, thereby enhancing their electrical efficiency. The maximum temperature observed in the glass, PV cell, wax, and nanofluid were 43.1°C, 42.35°C, 41.23°C, and 39.48°C, respectively, indicating efficient heat transfer within the system tabulated in Table 5. The reduction in temperature fluctuations, as shown in Figure 6 to Figure 9, highlights the role of NePCM in stabilizing the system's thermal performance. The nanoparticles in the wax and fluid significantly improve heat transfer, leading to higher output temperatures and overall system efficiency.

Table 5
Summary Table of Main Simulation Results

Parameter	Standalone PV	PVT-NePCM-Nanofluid (Observed)	PVT-NePCM-Nanofluid (Theoretical)
Glass Temperature (°C)	69.8	43.1	42.6
PV Cell Temperature (°C)	69.8	42.35	42.6
Wax Temperature (°C)	-	41.23	41.8
Nanofluid Temperature (°C)	-	39.48	39.5
Electricalefficiency (%)	15	14	14.50
Thermalefficiency (%)	-	69.40	70

The superior performance of the PVT-NePCM-nanofluid system is attributed to the enhanced thermal conductivity of the nanofluids and the latent heat storage capability of the NePCM. These materials effectively reduce the operating temperature of the PV cells, thereby improving electrical efficiency. However, the initial cost of nanomaterials and the complexity of maintaining an optimal nanofluid concentration are significant limitations. Future research should focus on cost-effective nanomaterials and automated systems for controlling nanofluid concentration to address these challenges.

4. Conclusions

The PVT-NePCM-nanofluid system demonstrated significant enhancements in both thermal and electrical performance. The experimental validation closely matched the theoretical model, with deviations of 3.72% and 5.05% for electrical and thermal efficiencies, respectively. The overall system efficiency improved to 84.5%, highlighting its potential for high-temperature applications. The primary limitations include the initial cost of nanomaterials and the need for precise control of nanofluid concentrations. Future research should optimize the nanofluid composition and explore alternative PCM materials to enhance system performance and reduce costs.

Acknowledgment
The author would like to thank S P Deshmukh, Institute of Chemical Technology.

References
[1] U.S. Energy Information Administration. "International Energy Outlook 2016." *EIA*, 2016.
[2] Solar Power Europe. "Global Market Outlook for Solar Power 2019-2023." *SolarPower Europe*, 2019.
[3] Rújula, Angel Antonio Bayod. *Sistemas fotovoltaicos*. Universidad de Zaragoza, 2009.
[4] National Renewable Energy Laboratory. "Champion Module Efficiencies Module Efficiency Chart." *NREL*, 2019.
[5] Smith, Brittany L., and Robert M. Margolis. *Expanding the photovoltaic supply chain in the United States: opportunities and challenges*. National Renewable Energy Laboratory, NREL/TP-6A20-73363, 2019. https://doi.org/10.2172/1547262

[6] Lorenz, Elke, Thomas Scheidsteger, Johannes Hurka, Detlev Heinemann, and Christian Kurz. "Regional PV power prediction for improved grid integration." *Progress in Photovoltaics: Research and Applications* 19, no. 7 (2011): 757-771. https://doi.org/10.1002/pip.1033
[7] Wysocki, Joseph J., and Paul Rappaport. "Effect of temperature on photovoltaic solar energy conversion." *Journal of Applied Physics* 31, no. 3 (1960): 571-578. https://doi.org/10.1063/1.1735630
[8] Hussien, Hashim A., Ali H. Noman, and Abdulmunem Raad Abdulmunem. "Indoor investigation for improving the hybrid photovoltaic/thermal system performance using nanofluid (Al_2O_3-water)." *Engineering and Technology Journal* 33, no. 4A (2015): 889-901. https://doi.org/10.30684/etj.33.4A.12
[9] Bigorajski, Jarosław, and Dorota Chwieduk. "Analysis of a micro photovoltaic/thermal-PV/T system operation in moderate climate." *Renewable Energy* 137 (2019): 127-136. https://doi.org/10.1016/j.renene.2018.01.116
[10] Kazemian, Arash, Mohammad Hosseinzadeh, Mohammad Sardarabadi, and Mohammad Passandideh-Fard. "Experimental study of using both ethylene glycol and phase change material as coolant in photovoltaic thermal systems (PVT) from energy, exergy and entropy generation viewpoints." *Energy* 162 (2018): 210-223. https://doi.org/10.1016/j.energy.2018.07.069
[11] Nasrin, Rehena, Nasrudin Abd Rahim, Hussain Fayaz, and Md Hasanuzzaman. "Water/MWCNT nanofluid based cooling system of PVT: Experimental and numerical research." *Renewable Energy* 121 (2018): 286-300. https://doi.org/10.1016/j.renene.2018.01.014
[12] Cuce, Erdem, and Pinar Mert Cuce. "Improving thermodynamic performance parameters of silicon photovoltaic cells via air cooling." *International Journal of Ambient Energy* 35, no. 4 (2014): 193-199. https://doi.org/10.1080/01430750.2013.793481
[13] Cuce, Erdem, Chin-Huai Young, and Saffa B. Riffat. "Performance investigation of heat insulation solar glass for low-carbon buildings." *Energy Conversion and Management* 88 (2014): 834-841. https://doi.org/10.1016/j.enconman.2014.09.021
[14] Sharaf, Omar Z., and Mehmet F. Orhan. "Concentrated photovoltaic thermal (CPVT) solar collector systems: Part I-Fundamentals, design considerations and current technologies." *Renewable and Sustainable Energy Reviews* 50 (2015): 1500-1565. https://doi.org/10.1016/j.rser.2015.05.036
[15] Moharram, Khaled A., M. S. Abd-Elhady, H. A. Kandil, and H. El-Sherif. "Enhancing the performance of photovoltaic panels by water cooling." *Ain Shams Engineering Journal* 4, no. 4 (2013): 869-877. https://doi.org/10.1016/j.asej.2013.03.005
[16] del Amo, Alejandro, Amaya Martínez-Gracia, Angel A. Bayod-Rújula, and Javier Antoñanzas. "An innovative urban energy system constituted by a photovoltaic/thermal hybrid solar installation: Design, simulation and monitoring." *Applied Energy* 186 (2017): 140-151. https://doi.org/10.1016/j.apenergy.2016.07.011
[17] Al-Nimr, Moh'D. A., and Moh'd-Eslam Dahdolan. "Modeling of a novel concentrated PV/T distillation system enhanced with a porous evaporator and an internal condenser." *Solar Energy* 120 (2015): 593-602. https://doi.org/10.1016/j.solener.2015.08.006
[18] Sheikholeslami, M. "Numerical investigation for concentrated photovoltaic solar system in existence of paraffin equipped with MWCNT nanoparticles." *Sustainable Cities and Society* 99 (2023): 104901. https://doi.org/10.1016/j.scs.2023.104901
[19] Sheikholeslami, M., and Z. Khalili. "Simulation for impact of nanofluid spectral splitter on efficiency of concentrated solar photovoltaic thermal system." *Sustainable Cities and Society* 101 (2024): 105139. https://doi.org/10.1016/j.scs.2023.105139
[20] Duffie, John A., and William A. Beckman. Solar engineering of thermal processes. John Wiley and Sons, 1991.
[21] Kumar, Suresh, and S. C. Mullick. "Wind heat transfer coefficient in solar collectors in outdoor conditions." *Solar Energy* 84, no. 6 (2010): 956-963. https://doi.org/10.1016/j.solener.2010.03.003
[22] Incropera, Frank P., David P. Dewitt, Theodore L. Bergman, and Adrienne S. Lavine. *Principles of Heat and Mass Transfer: International Student Version*. John Wiley & Sons., 2011.
[23] Farshchimonfared, M., J. I. Bilbao, and A. B. Sproul. "Full optimisation and sensitivity analysis of a photovoltaic-thermal (PV/T) air system linked to a typical residential building." *Solar Energy* 136 (2016): 15-22. https://doi.org/10.1016/j.solener.2016.06.048
[24] Aqilah, Nur, Khizar Ahmed Pathan, and Sher Afghan Khan. "Passive Control of Base Flow at Supersonic Mach Number for Area Ratio 4." In *International Conference on Advances in heat Transfer and Fluid Dynamics*, pp. 37-50. Singapore: Springer Nature Singapore, 2022. https://doi.org/10.1007/978-981-99-7213-5_4